Fundamental Diagram of Traffic Flow

New Identification Scheme and Further Evidence from Empirical Data

Jia Li and H. Michael Zhang

A systematic approach is developed to identify the bivariate relation of two fundamental traffic variables, traffic volume and density, from single-loop detector data. The approach is motivated by the observation of a peculiar feature of traffic fluctuations. That is, in a short time, traffic usually experiences fluctuations without a significant change in speed. This fact is used to define equilibrium in a new manner, and a mixed integer programming approach is proposed for constructing a piecewise linear fundamental diagram (FD) accordingly. By construction, the proposed method is data adaptive and optimal in the sense of least absolute deviation. This method is used to perform a case study with data from one section of a multilane freeway. The results indicate that both capacity drop and concave–convex FD shapes abound in practice. Differences in traffic behavior across freeway lanes and along freeway sections revealed through the FD are discussed.

The fundamental diagrams (FDs), that is, bivariate equilibrium relationships of traffic flow, concentration, and speed, are of great theoretical and practical concern. For example, the concept of level of service for a highway is based on the speed–flow FD. FDs are also of particular interest in their own right in traffic flow theory. The flow–density FD, for example, specifies the transition patterns of various traffic states on the phase plane and completes the kinematic wave (KW) traffic flow theory. In high-order models, the speed–density or speed-spacing FD also plays a critical role. Such models can be conveniently analyzed in the framework of the effective FD (*1*), which demonstrates from another perspective the rich information inherent in the FDs, as well as their importance in understanding and modeling traffic flow. Throughout the following discussion, FD specifically refers to the flow–density FD unless otherwise noted.

Numerous efforts have sought to identify FDs from observations. Early researchers searched for the best fit to data while implicitly assuming the existence of FDs (*2*). The existence of FDs was empirically and constructively confirmed by a series of later studies (*2–4*). These studies were similar in spirit: stationary measurement were extracted, and it was shown that these measurements form well-defined curves. Although a complete picture of traffic phase transitions is still unclear (*5*), the existence of FDs is widely acknowledged.

J. Li, 1001 Ghausi Hall, and H. M. Zhang, 2001 Ghausi Hall, Department of Civil and Environmental Engineering, University of California, Davis, 1 Shields Avenue, Davis, CA 95616. Corresponding author: H. M. Zhang, hmzhang@ucdavis.edu.

Transportation Research Record: Journal of the Transportation Research Board, No. 2260, Transportation Research Board of the National Academies, Washington, D.C., 2011, pp. 50–59.
DOI: 10.3141/2260-06

This paper further investigates the specification and calibration of FDs. The purpose is to provide a consistent, systematic, and adaptive way to obtain FDs from single-loop detector measurements. In particular, the piecewise linear form is adopted for the FD, because (*a*) more-complex forms of the FD can be approximated by a piecewise linear form with arbitrarily many pieces, and (*b*) empirical evidence tends to support such a form. For example, Windover and Cassidy found that there is no dependency of wave speed on flow in either the free-flow or the congested region of traffic, implying that the flow–density relationship is locally linear (*6*). Meanwhile, the piecewise linear form greatly simplifies analysis and computation of the kinematic wave model of Lighthill and Whitham (*7*) and Richards (*8*). For example, explicit calculation is enabled in Newell's simplified KW theory (*9*) and the cell transmission model (*10*) with the use of triangular or trapezoidal FDs.

RELATED WORK

Castillo and Benítez derived a functional form for the speed–density relation as the solution to a system of mathematical and behavioral constraints (*2*). Among these constraints, the following three are essential: the speed–density relation $V(\rho)$ is sufficiently smooth, for example, $V(\rho) \in C^1$; speed is a decreasing function of density, that is, $V'(\rho) < 0$; and the flow–density relation is concave, that is, $Q''(\rho) < 0$. In the accompanying empirical study (*11*), calibration of the proposed FD is based on a method to identify stationary states.

Like Castillo and Benítez (*11*), Cassidy suggested that the stationary traffic state is marked by constant average vehicle speeds and a linear trend in cumulative vehicle arrivals (*4*). The near-stationary periods are identified through careful examination of the cumulative curves. Then the identified near-stationary traffic data are averaged over 4- to 10-min periods to suppress the random fluctuations. The averaged data form a curve, implying the existence of FDs.

Pertaining to the previous two studies, Coifman formulated the problem of traffic measurement smoothing in a unified perspective of digital filtering design (*3*). It was observed that the common approaches to eliminating noise in traffic measurements, for example, fixed time average, moving average, and cumulative summation, can all be formulated as equivalent filter forms in the frequency domain.

The preceding methods are all trend oriented; that is, they rely on the trend of measurements to identify the stationary states and construct FDs. However, studies indicate that congested traffic cannot maintain stationarity for a prolonged period (*4, 11*). Therefore, the constructed FD contains many observations only in high-occupancy regions. It is also not clear whether $Q(\rho)$ should be concave, as

hypothesized by Castillo and Benítez (*2*). Arguably, only in this case does the Lighthill–Whitham–Richards model render "solutions with deceleration shock waves" (*2*). However, substantial empirical evidence has contradicted this hypothesis (*12, 13*).

NEW IDENTIFICATION SCHEME

Throughout the following discussion, it is assumed that the conversion between occupancy (percent) and traffic density is defined by affine mapping: density = 200 × occupancy. This relation is equivalent to the constant *g*-factor assumption for velocity estimation, essentially stating that the effective vehicle length is constant over time. Apparently restrictive, this assumption agrees with reality well, especially during peak periods (*14*). The variation in the *g*-factor is mainly caused by the appearance of heavy trucks; therefore, their influences are most significant on morning or night right-lane traffic.

The following notation is used:

d = detector length,
Δt = sampling interval,
i = sampling time,
j = detector,
q_{ij} = flow measurement, and
occ_{ij} = occupancy measurement.

Index may be dropped when no confusion arises.

There are two key differences between this approach and previous approaches. First, the concept of equilibrium is examined more carefully. For a complex system like traffic, the equilibrium is inevitably accompanied by fluctuations. This study conjectures that fluctuation features reveal information such as deviation of traffic from equilibrium. This leads to a detrended fluctuation analysis elaborated on later in the paper. Second, the piecewise linear functional form was chosen for FD. Such a selection allows for sufficient flexibility to capture curious patterns in the FD while remaining simple enough to allow quick solution of corresponding KW problems. With trapezoidal and triangle FD as special cases, the piecewise linear FD encompasses much richer modeling possibilities. The KW problem with piecewise linear FD is locally a linear advection equation, and its solution can be analytically given when the FD stays continuous (*15*).

Motivating Observation: Peculiarity of Traffic Fluctuations

Traffic is characterized by the first as well as high-order information of its fundamental variables. Experimental study found a simultaneous decrease of mean velocity and increase of variance of velocity with traffic jam (*16*). This was also indirectly revealed by Coifman (*3*) and Cassidy (*4*), that is, congestion traffic is subject to larger variability. Therefore, there is a strong sign indicating the fundamental difference between congested and free-flow traffic for fluctuation patterns. This observation motivates the development of an identification method to differentiate traffic states, based on not only trend but also fluctuation characteristics.

Fluctuations are closely related to time scale, which can be several minutes, hours, or days. Associated with the concept of time scale, some attention has been paid to the scaling properties of traffic (*17*). ("Scaling property" refers to traffic properties with explicit dependency on the time scale of description.) Although the existence of and underlying reasons for scale-invariant properties of traffic remain to be explored, the existence of various characteristic time scales appears to be well recognized.

Fluctuations of the intermediate frequency, that is, those induced by stop-and-go traffic and that persist several minutes, are among the most elusive traffic phenomena. This type of fluctuation was extensively observed and analyzed (*18–20*). This is called traffic oscillations when the focus is on spatial propagation of disturbances. At the upstream locations of a freeway section, the oscillations of all traffic variables have largely the same dominating frequency of 2 to 3 mHz, corresponding to a period of 5 to 8 min (*20*).

For bivariate fluctuations of traffic states on the flow–density phase plane, the conventional one-dimensional data analysis tools, such as Fourier transformation and cumulative curve analysis, are not applicable. Therefore, an adaptive aggregation algorithm was developed to facilitate the analysis. The spirit of this algorithm is simple: consecutive measurements are aggregated if they lie in a small neighborhood. With such treatment, the local random fluctuations are suppressed, and traffic state transition patterns are more visually identifiable. The adaptive approach is less likely to introduce spurious states and thus is more effective in exploiting traffic peculiarities.

With the aggregation scheme and 30-s middle-lane count-occupancy data from one section of eastbound I-80 near Davis, California, an empirical plot along with its schematic representation were obtained, as shown in Figure 1. Here the neighborhood is defined as a rectangle of size 2×0.1. Although this neighborhood size is not expected to be optimal, this setting helps one visualize and interpret data that in raw form is very noisy. The patterns shown in Figure 1 are common to other data sets. For congested traffic, there are two major types of transitions. In a region with very high occupancy, loops commonly known as hysteresis are observed. The other type of transition gradually becomes dominant when traffic becomes less congested, that is, when occupancy is not as high. In contrast to hysteresis, these transitions occur primarily along straight lines emanating from the origin of the traffic count–occupancy plane. As mentioned, the *g*-factor is nearly constant in congestion region. Therefore, the straight lines correspond to traffic of constant speed, and these transitions are called speed-constant fluctuation.

In addition to the intuitive proof in Figure 1, a more rigorous empirical justification to the existence of speed-constant fluctuations is as follows. Mathematically, a process consists of speed-constant fluctuations if and only if it satisfies the condition

$$\frac{\text{count}_i}{\text{occ}_i} = \frac{\Delta\text{count}_i}{\Delta\text{occ}_i} \qquad \forall i \in N \tag{1}$$

where

Δ = forward difference operator, that is, $\Delta f_i = f_{i+1} - f_i$ for a given series f_i;
count_i = traffic count in the ith sampling period;
occ_i = occupancy in the ith sampling period; and
N = set of natural numbers.

The left column of Figure 2 shows calculated values of the left and right sides of Equation 1 done with two data sets, which are preconditioned with the adaptive aggregation algorithm. The units of count/occ and Δcount/Δocc are vehicles per 30 s. The negative Δcount/Δocc are not shown in the figure because they pertain to hysteresis. The hysteresis states are also relatively few. In the lower left graph, for example, of the 242 aggregated traffic states during hours of congestion (3:00 to 8:00 p.m.), only 12 (4.96%) pertain to hysteresis transitions. In the left column of Figure 2, the profiles of Δcount/Δocc and count/occupancy are very alike in general trend,

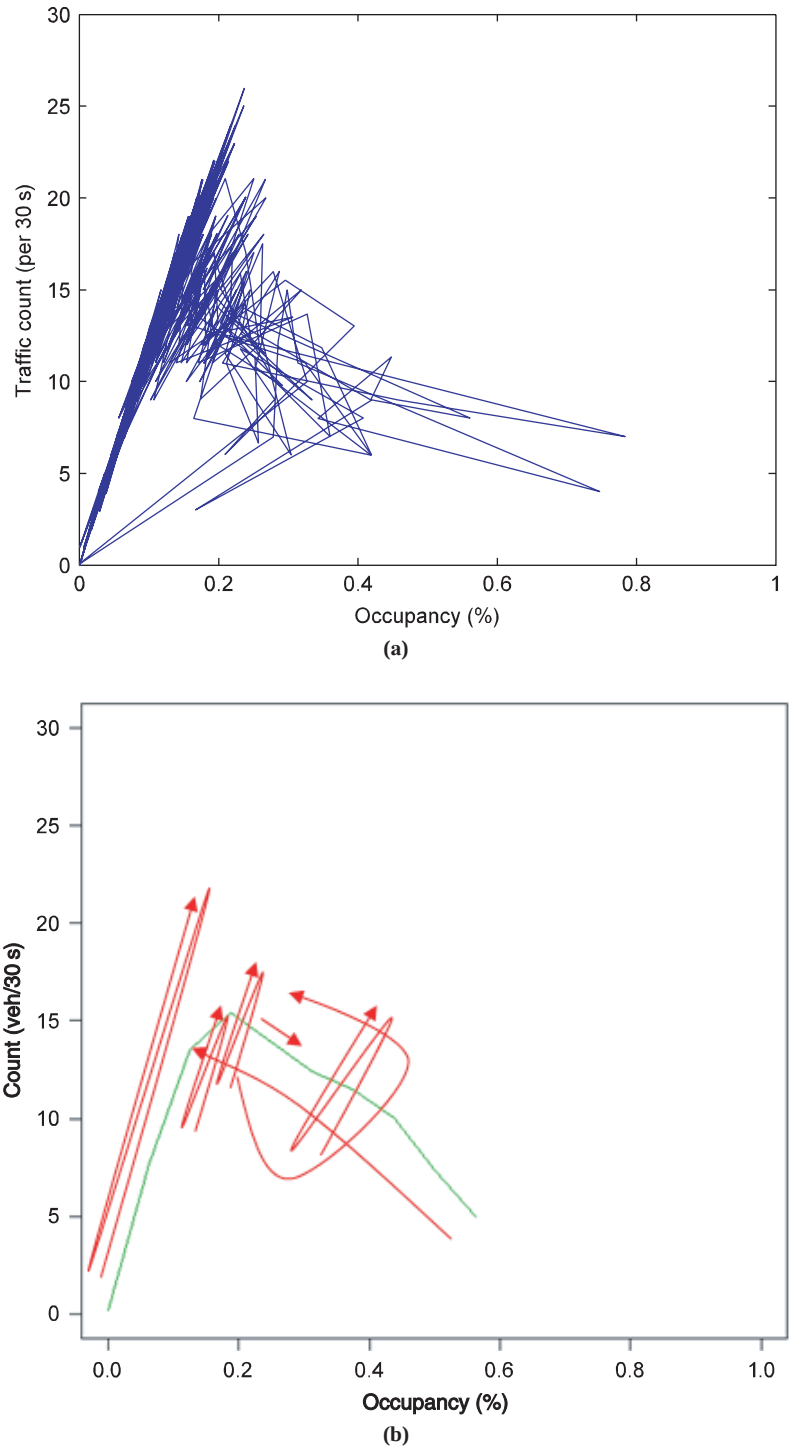

FIGURE 1 (*a*) Empirical and (*b*) schematic representations of transition patterns on traffic count–occupancy phase plane.

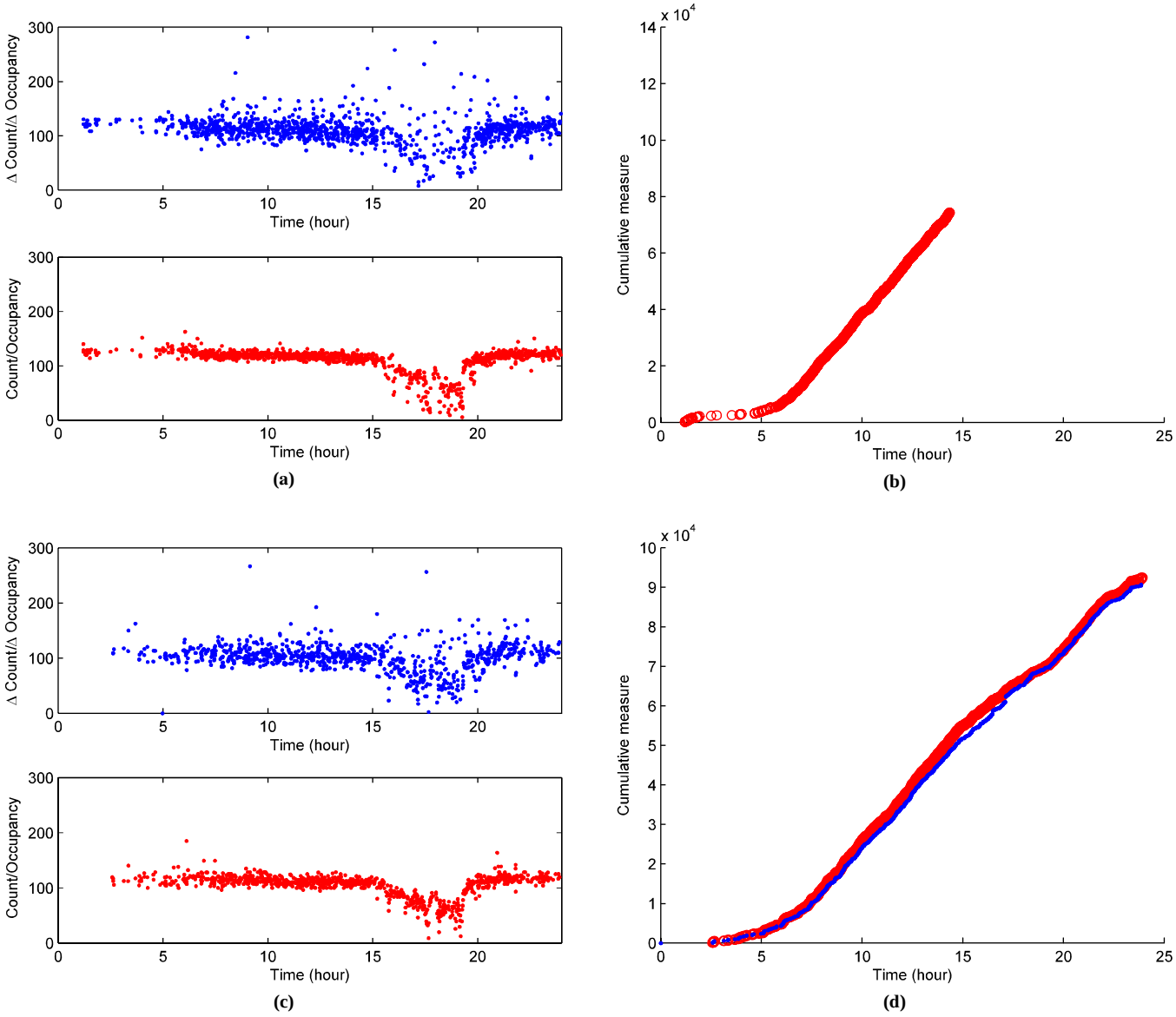

FIGURE 2 Empirical evidence justifying conjecture of speed-constant fluctuation.

except that the former appears slightly more scattered, indicating it is more sensitive to data variations. The following cumulative measures are used to compare the trend of two profiles in a more evident manner:

$$m_1(i) = \sum_{s \le i} \frac{\text{count}_s}{\text{occ}_s} \quad \text{and} \quad m_2(i) = \sum_{s \le i} \frac{\Delta\text{count}_s}{\Delta\text{occ}_s} \tag{2}$$

where

m_1 and m_2 = cumulative measures,
count_s = traffic count in the sth sampling period, and
occ_s = occupancy in the sth sampling period.

The slopes of these measures are roughly proportional to the instantaneous traffic speed under the assumption of constant g-factor. The right column of Figure 2 presents the calculation results, each graph corresponding to its left neighbor. The curves m_1 and m_2 are plotted with a thick red line and a thin blue line, respectively. A very good match of the m_1, m_2 profiles is found in both cases. This finding further justifies the validity of Equation 1. Hence the conjecture of constant-speed fluctuation holds.

An explanation of the speed-constant fluctuation is that drivers are usually reluctant to change their speeds when possible. (In the long run they are still subject to the equilibrium relation, especially in heavy traffic.) Thus, a perturbation such as a slowdown will induce a change of the space gap between leading and following vehicles, and thus of flow rate, but not necessarily the speed, for a short period before the gap between vehicles is too small for that traveling speed.

Structure of FDs

With the observation that speed-constant fluctuations are dominant, it is postulated that a FD has the structure shown in Figure 3. The

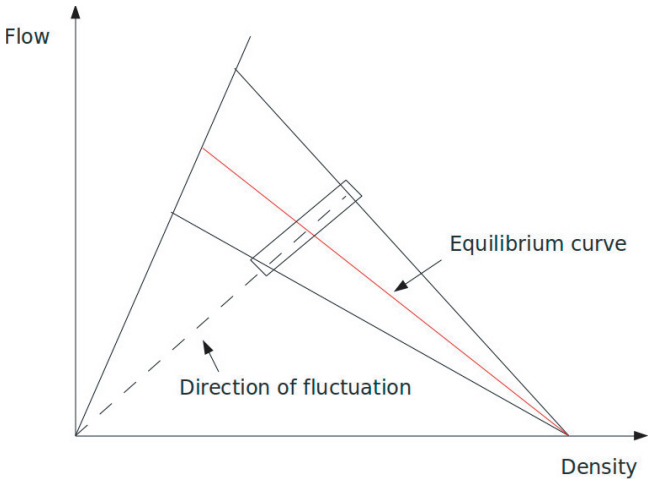

FIGURE 3 Postulated structure of FD.

free-flow branch is a single line, and the congestion branch is a fan consisting of many line segments emitting from the origin, which represent the speed-constant fluctuations. The red line illustrates the equilibrium states associated with the congestion state fluctuations, per the new definition elaborated later. A complete characterization of all transition details associated with FD is beyond the scope of this paper; relevant discussions are available elsewhere (*1*).

Identifying Equilibrium States: Minimum Principle

The first step in FD construction is to split the free-flow data from congested-flow data. First define a measure of fluctuation strength, called the fluctuation index:

$$p_f(i) = \frac{\lambda}{w}\sqrt{\sum_{A=\{s:|s-i|\Delta t<w\}}\left(f(s)-f_{\mathrm{loc}(A)}(s)\right)^2} \tag{3}$$

where

f = time series of interest,
$f_{loc(A)}(\cdot)$ = local linear approximation of $f(\cdot)$ on set A in the least-squares sense,
w = bandwidth parameter that needs to be prescribed,
λ = scaling parameter nondimensionalizing the whole term, and
s = sth sampling period.

By construction, the measure p_f is dimensionless and independent of the trend of data. The first property means the fluctuation index is invariant with respect to the change of measurement unit. As such, fluctuation indices based on data of different aggregation levels are comparable. The second property is desirable because when the series under analysis are nonstationary, the trend values may smear the information carried by the high-order characteristics of data. The detrended fluctuation analysis, whose theoretical rationale is similar, is discussed elsewhere (*21*). The value of λ is specified such that $< p_f \geq 1$ over the course of observation. Therefore, λ is calculated as

$$\lambda = \frac{nw}{\sum_i \sqrt{\sum_{A=\{s:|s-i|\Delta t<w\}}\left(f(s)-f_{\mathrm{loc}(A)}(s)\right)^2}} \tag{4}$$

where n is the total number of observations. Specification of w is an ad hoc issue; it should be small enough to reflect the local fluctuation features while being large enough to cover at least several state transitions. The adaptive aggregation algorithm was used to find that the average gap between consecutive state transitions was about 1.5 min (calculated as the total observation time divided by number of aggregated states). Therefore, a time window of 5 to 10 min should be appropriate. Moreover, experiments with a set of values of w in this range do not indicate strong numerical difference, so $w = 5$ min here.

The profiles of fluctuation index appear noisy in its original form (Figure 4*a*), but some important features are still identifiable. The onset of congestion is accompanied by stronger fluctuations in occupancy but weaker fluctuations in traffic count. This observation

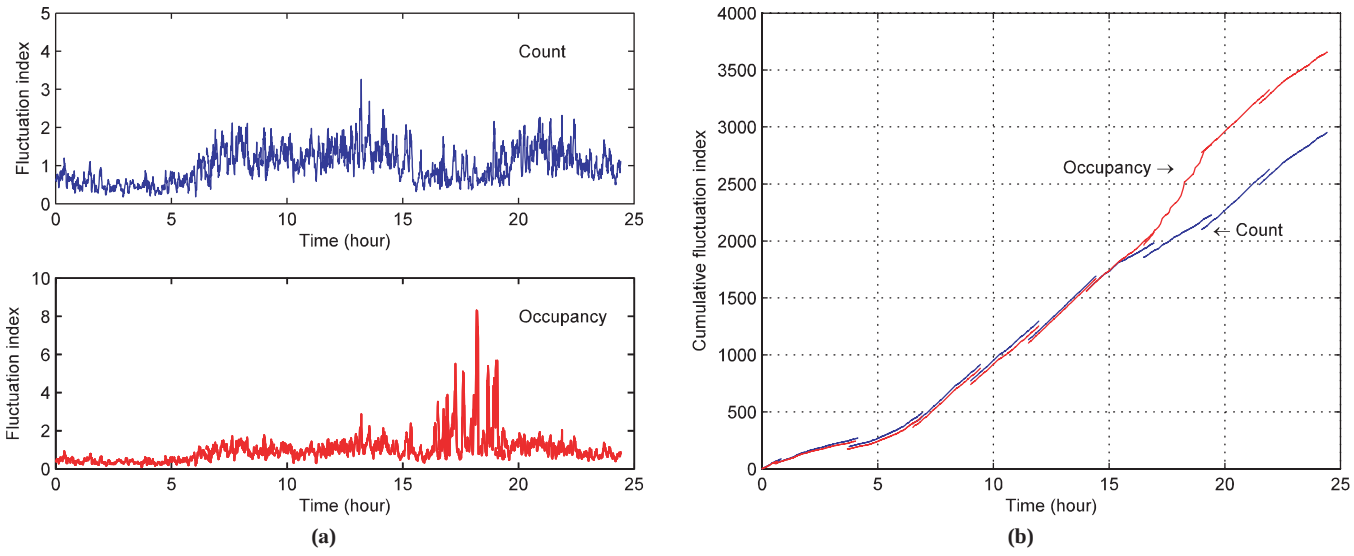

FIGURE 4 Comparison of fluctuation indices during 1 day: (*a*) original form and (*b*) cumulative form.

is consistent with stop-and-go traffic, which tends to maintain a steady flow although an individual's driving experience is less uniform. The patterns of fluctuations are shown more clearly by the cumulative fluctuation profile, defined as the fluctuation index integrated over time (Figure 4*b*). In this graph, the cumulative fluctuation profile of occupancy is rescaled by a constant factor 1.25. This treatment allows the two cumulative profiles to overlap each other nicely until congestion onset (around 3:00 p.m.). After the congestion is fully dissipated (around 8:00 p.m.), the two profiles again increase with the same rate.

This finding implies that the fluctuations of occupancy and traffic count are proportional unless traffic is congested. To capture this effect, a traffic state indicator $c(i)$ is defined as the corrected ratio of the two fluctuation profiles p_{count} and p_{occ},

$$c(i) = \min\left\{\frac{\max\{p_{\text{occ}}(i), \epsilon\}}{\max\{p_{\text{count}}(i), \epsilon\}}, C\right\} \tag{5}$$

Definition as such avoids numerical problems in calculation: ϵ is a small number to exclude a zero denominator, and the constant C ensures that $c(i)$ is upper bounded by a reasonable value; $\epsilon = 10^{-3}$, $C = 10$. The $c(i)$ can be clustered with the K-means approach. The number of clusters is two, corresponding to the free and the congested traffic, respectively. Figure 5 is an example of the resulting state split. The figure shows that the developed measure effectively separates the traffic phases: high-occupancy traffic and low-occupancy traffic are clearly distinguished. Despite this, traffic of intermediate occupancy can fall into both categories. This is possibly because of the sensitivity of the proposed indicator to the relatively large variation in raw data.

Equilibrium can be obtained by suppressing the high-frequency components of traffic data and then identifying the constant periods. However, the stationarity criterion usually needs to be relaxed for a constant period of congested traffic to be found. This indicates a fundamental deficiency of defining equilibrium via stationarity criterion, because congested traffic is seldom stationary. Therefore, it is desirable to define equilibrium states in an alternative way. This problem is approached by defining the equilibrium states through a minimum principle: the equilibrium FD is a curve consisting of points (density, flow) = (k_e, f_e) such that the speed-constant fluctuations around point (k_e, f_e) are symmetric with respect to the FD, that is, the difference of possibilities to visit each side of an equilibrium curve is minimal. The philosophical consideration underlying this definition is that fluctuations should be symmetric to the equilibrium, unless disproved. This definition is empirically sound because of the dominance of speed-constant fluctuation demonstrated earlier. Moreover, in a modeling perspective, a solution of a kinematic wave problem with FD obtained as such should be unbiased with respect to the real scattered data.

Given this definition, there should be an equal number of observations on both sides of an equilibrium curve in the direction of constant speed. For any given density k_e, the following algorithm is proposed to obtain the corresponding f_e. This algorithm uses simple geometry relations illustrated in Figure 3: for a given k_e, iteratively search for a corresponding f_e that is median to all observations in a speed-constant region (the small rectangle in Figure 3). It reads as follows:

1. Set initial guess of f_e : $f_e = f_0$.
2. Rotate the observation on the phase plane counterclockwise by $(\pi/2) - \theta$ with respect to (k, f_e), where $\theta = \arctan(f_e/k)$. Denote the rotated set as B_{rot}.
3. Calculate the median of $\{f' : (k', f') \in B_{\text{rot}}, |k' - k| < w_k\}$, where w_k is a parameter specifying the width of rectangle illustrated in Figure 3. Denote it as f_m.
4. Check if $|f_e - f_m| \le \epsilon$, where ϵ is a prescribed threshold parameter. If so, stop the calculation and return value f_e; otherwise, set $f_0 = f_m$ and go to Step 1.

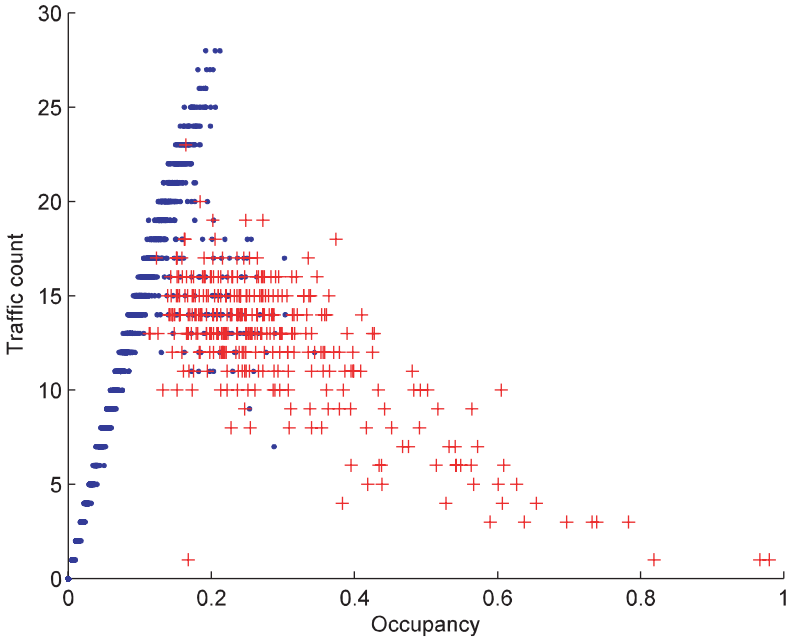

FIGURE 5 Split of observations. Dots indicate free flow; plus signs indicate congested flow.

Congested traffic data are used to apply this algorithm with $w_k = 10$ min. w_k cannot be too small; otherwise, the set in Step 3 may be empty. The smallest w_k that ensures the algorithm runs without premature termination is chosen. For free-flow traffic, similar to previous studies, the equilibrium state can be obtained by simply taking time averages. The time window was set at 20 min, because the smoothing result does not have strong dependency on this value.

Adaptive Piecewise Linear Fit

When data of equilibrium states are obtained, it is desirable to obtain a functional form that neatly describes them. Compared with a fixed functional form, a nonparametric form is more favorable, because the latter is data driven and thus much more flexible. The fit that has the least absolute deviation is preferred, because such a fit is insensitive to outliers in measurement.

The FD fitting method is based on a generic formulation proposed by Bertsimas and Shioda (*22*), which seeks the piecewise linear fit of data with least absolute deviation via a mixed integer program. The FD fitting method is as follows. Denote $(\text{occ}_i, \text{count}_i) = (x_i, y_i)$, $i = 1, \ldots, N$ the set of observations. Without loss of generality, assume $x_1 \le \cdots \le x_N$. The following program solves the best m-piece linear description (which possesses the least absolute deviation) of this set of data: $y = \beta_j x + \gamma_j$, $j = 1, \ldots, m$, $x \in D_j$, where $\{D_j, j = 1, \ldots, m\}$ is a partition of the set $\{x_1, \ldots, x_N\}$ satisfying $\max D_i \le \min D_{i+1}$, $i = 1, \ldots, N-1$. The program reads

$$\min \sum_{i=1}^{N} \delta_i$$

such that

$$\delta_i \ge \left(y_i - \beta_j x_i - \gamma_j\right) - M\left(1 - a_{ij}\right) \quad i = 1, \ldots, n;\ j = 1, \ldots, m \qquad (c1)$$

$$\delta_i \ge \left(-y_i - \beta_j x_i - \gamma_j\right) - M\left(1 - a_{ij}\right) \quad i = 1, \ldots, n;\ j = 1, \ldots, m \qquad (c2)$$

$$\sum_{j=1}^{m} a_{ij} = 1 \quad i = 1, \ldots, n \qquad (c3)$$

$$a_{ij} + a_{i'j'} \le 1 \quad i = 1, \ldots, n;\ j = 1, \ldots, m;\ i' \le i;\ j' > j \qquad (c4)$$

$$a_{ij} + a_{i'j'} \le 1 \quad i = 1, \ldots, n;\ j = 1, \ldots, m;\ i' \ge i;\ j' < j \qquad (c5)$$

$$a_{ij} \in \{0, 1\} \quad i = 1, \ldots, n;\ j = 1, \ldots, m \qquad (c6)$$

$$\gamma_1 = 0 \qquad (c7)$$

(6)

In this formulation, the decision variables are δ_i and a_{ij}; m is a sufficiently large number. The a_{ij} is binary (Constraint *c*6), which equals 1 if observation i is fitted by the jth piece and 0 otherwise. The continuous δ_i model the deviation of the ith observation to the fit via Constraints *c*1 and c2. Constraint *c*3 says that each observation corresponds to one and only one piece of fit. Constraints *c*4 and *c*5 ensure that each piece covers the points in an interval. Constraint *c*7 ensures that free-flow branch passes origin on the phase plane.

Constraints *c*4 and *c*5 also enforce that the resulting fit is a well-defined (i.e., single-valued) function, although not necessarily continuous. Removal of these two constraints could result in a fit with multiple y corresponding to one x, for example, a reverse-λ FD (*12*). Parameter m needs to be specified. This largely determines what the fitted FD look like. When m is large, the resulting FD virtually approximates any relationship that is not necessarily continuous or concave. It is possible to determine an optimal m by minimizing certain objective functions, which consist of the fitting deviation and penalty caused by larger m. Nonetheless, physical interpretability and computational simplicity should be more of more concern in the context of the traffic flow problem.

Treatment of Tail

Usually, the observed sample near very high density is quite limited. This prevents reliable estimation of the FD in this region. Castillo and Benitez suggested that the wave speed c_j at jam density is a relatively consistent value around −15 mph (*11*). For a particular site, ideally, this value can be estimated as the maximizer of a cross-correlation-based value of measurement at two consecutive sites, that is,

$$\hat{c}_j = -\frac{d_{ud}}{\arg\max_j \sum_{n=1}^{N-j} x_{n+j}^{(u)} x_n^{(d)} \Delta t} \qquad (7)$$

where

$x_{n+j}^{(u)}$ = upstream measurement,
$x_n^{(d)}$ = downstream measurement, and
d_{ud} = distance between these two sites.

Calculations revealed an issue in applying Formula 7 when $d_{ud}/\Delta t > c_j$. This is because the sampling rate does not warrant sufficient resolution. In this case, the following estimate is adopted:

$$\hat{c}_j = -\frac{f\left(\max k_e\right)}{k_j - \max k_e} \qquad (8)$$

where f represents the piecewise linear fit to the data. It must be double-checked that Equation 8 produces values consistent with a priori knowledge. The values $c_j \in [8,15]$ mph are reasonable (*11*).

Following is a summary of the steps needed to obtain the flow–density FD from single loop detector measurements:

1. Transform the occupancy and traffic count data to traffic density and traffic flow data.
2. Separate the two traffic states based on fluctuation characteristics.
3. Use the minimum principle to identify representative equilibrium points.
4. Fit the equilibrium data with a piecewise linear function.
5. Treat the tail with estimated c_j.

Although quantitative results will rely on the selection of the conversion factor between occupancy and density, that is, the g-factor, its specific value does not affect Steps 2 and 3. Moreover, the shape of the fitted FD is independent of the g-factor as long as the affine relation of occupancy and flow is kept, because a change in g-factor is equivalent to a relabeling of the horizontal axis of the flow–density plane.

CASE STUDY

The preceding method is applied to real data in this section. The data used are freeway loop detector measurements of eastbound traffic from a 2.5-mi segment of I-80 located between Davis and Sacramento,

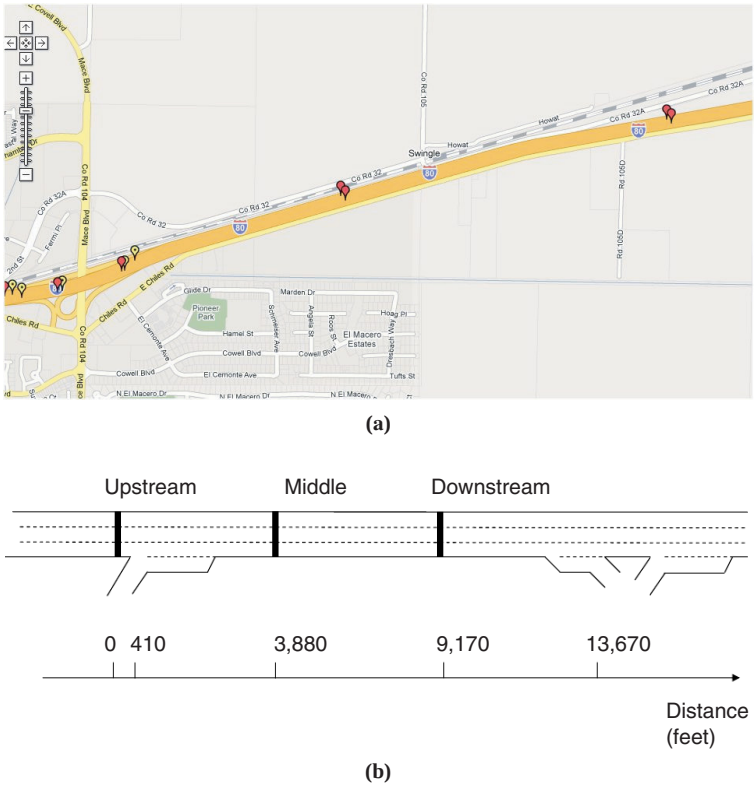

(a)

(b)

FIGURE 6 I-80 eastbound, Davis: (*a*) site map and (*b*) illustration of layout (not to scale).

California. The site map and layout are given in Figure 6. This freeway segment has three lanes. The upstream detector is located about 410 ft (0.07 mi) before an on ramp, and the downstream detector is located about 4,500 ft (0.85 mi) before an off ramp. Recurrent congestion occurs downstream of this segment around the off ramp on Friday afternoons. The congestion spills back and is observed at those detectors. Data from October 23, 2009, are used. The measurement interval is 30 s.

The method illustrated earlier is used to fit eight FDs with the measurements from the nine detectors (three lanes and three locations). The right lane in the upstream location is significantly influenced by the oncoming merging traffic from the on ramp, and its corresponding fluctuation characteristics are quite different from those of the others: even at low densities, the fluctuations at this site are as significant as those at highly congested densities. In such a case there is no clear transition between free flow and congested flow, and the method based on fluctuation strength does not apply. To accommodate the issue, the piecewise linear fit was applied to 20-min averages.

The fitting results are presented in Figure 7. The figure shows that the FDs at different locations in each lane have the same shape in general, whereas they differ significantly across lanes. The left-lane FDs consist of disconnected pieces, with a sudden drop in capacity at the critical density. This indicates that the transition from free flow to congested flow in this lane is quite sharp, without much wandering in the intermediate region. The middle-lane FDs are generally triangular, as typically assumed in modeling (*9, 10*). This is most evident in the downstream location of the middle lane. Some of the FDs in the middle- and left-lane locations are convex rather than concave in the congested branch, implying the existence of acceleration shocks and deceleration wave fans. The right-lane FDs appear most varied, especially at both the upstream and downstream locations where weaving is prominent. Closer to ramps, the right-lane FDs tend to have a gradual transition from free flow to congestion, hence a flatter top, which is a sign of the presence of a bottleneck. Away from ramps where lane-changing activities diminish, the right-lane FD has more or less a triangular shape. Regardless of location, the maximum flow decreases from left to middle to right lane.

Table 1 provides parameters and errors of the identified FDs. With the piecewise linear fit, the free-flow speed v_f, critical density k_1, and capacity f_{cap} are easily identified. Moreover, the wave speeds in congested regions, $c_j^{(1)}$ and $c_j^{(2)}$, are conveniently known. As commonly expected, free-flow speed v_f, critical density k_1, and capacity f_{cap} decrease from the left lane to the right lane. Absolute values of wave speed $c_j^{(2)}$ are also decreasing, but not as much as free-flow speed. The mean absolute error (MAE) of each FD fit is calculated; the MAE is the value of the objective function in Equation 6 divided by the number of identified equilibrium observations. MAE can be regarded as an uncertainty measure, indicating how well the data can be described by the proposed FDs. It is found that left-lane FDs tend to have larger MAE values. The upstream right-lane FD also has a large MAE value because of the uncertain data. Furthermore, relative mean absolute error (rMAE) is defined to eliminate the influence of scale. rMAE is obtained by dividing the MAE by value of capacity f_{cap}. The upstream right-lane FD is found to have an rMAE of 6%; rMAE values are 1.5% to 3% for all other FDs. This indicates that uncertainty pertaining to the upstream right lane is inherently large.

Although the presented method does not enforce the $c_j^{(2)}$ (shock wave speed at extremely high density) to be in a certain range, the

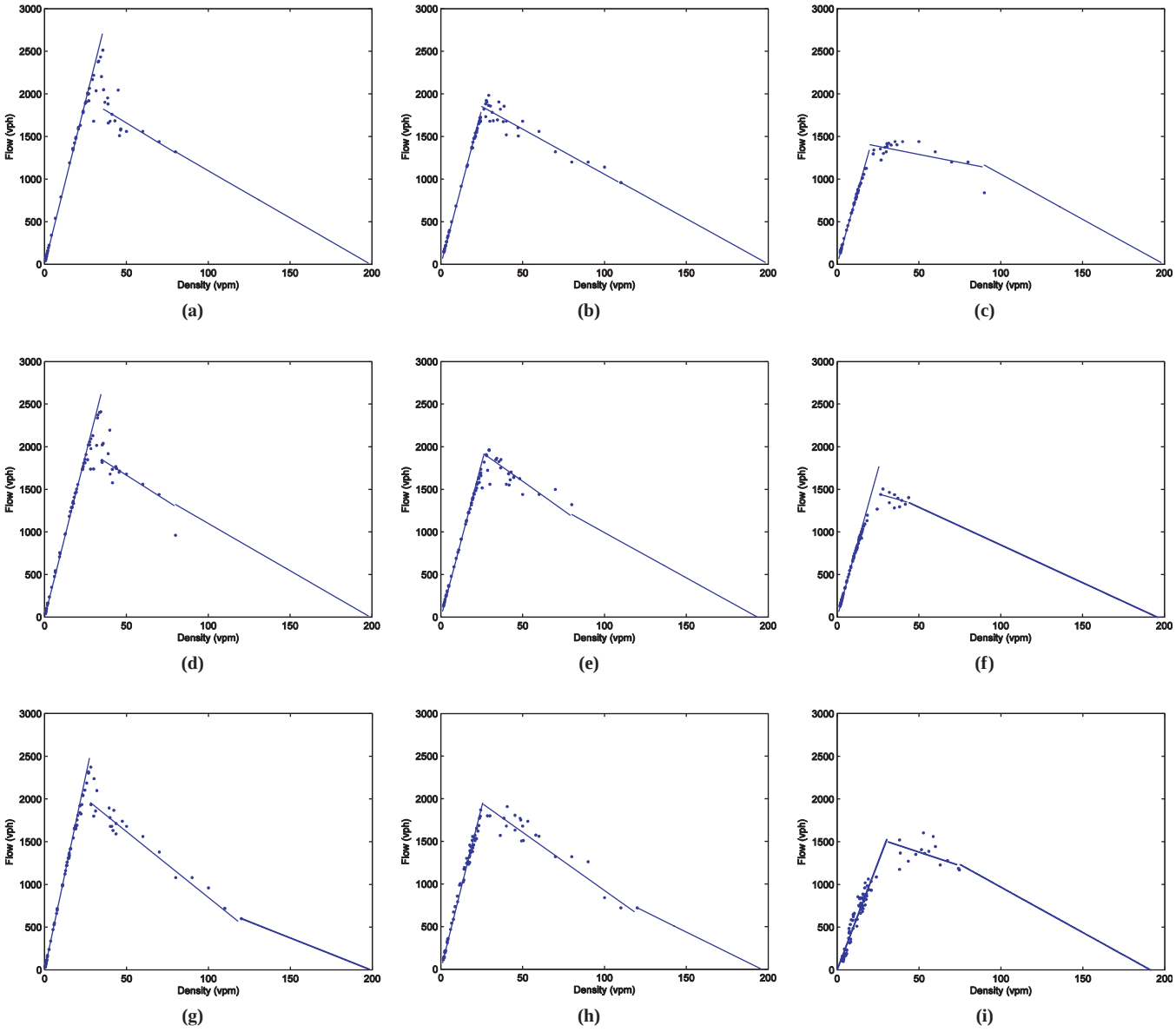

FIGURE 7 Identified FDs with I-80 data. Left to right: left lane to right lane; bottom to top: upstream to downstream.

TABLE 1 Parameters and Goodness of Fit of Piecewise Linear FDs

Lane	v_f (mph)	$c_j^{(1)}$(mph)	$c_j^{(2)}$(mph)	k_1 (vpm)	k_2 (vpm)	f_{cap} (vph)	MAE (vph)	rMAE (%)
Location: Upstream								
Left	88.4	−14.5	−7.6	28.3	120	2,495	43.1	1.7
Middle	75.1	−12.2	−9.0	26.4	120	1,993	57.5	2.9
Right	49.8	−6.0	−9.9	31.1	75	1,234	74.1	6.0
Location: Middle								
Left	75.1	−11.7	−11.0	34.7	80	2,608	64.1	2.5
Middle	70.8	−13.3	−10.0	27.1	80	1,920	43.7	2.3
Right	67.9	−5.4	−8.6	25.6	44	1,735	26.5	1.5
Location: Downstream								
Left	75.5	−11.4	−11.0	35.8	80	2,702	71.5	2.6
Middle	71.7	−10.5	−10.7	25.3	110	1,814	41.0	2.3
Right	67.2	−3.4	−10.6	20.0	90	1,343	32.5	2.4

results turn out to be consistent with observations summarized by Castillo and Benitez (*11*). This case study also lends empirical support to the choice of simple FDs, that is, FDs with a piecewise linear form: the piecewise linear form appears to fit data well, and the triangular form appears naturally in some cases, although a three-piece form is specified in the data fitting procedure.

CONCLUSIONS

This paper presented a method for identifying and calibrating a piecewise linear FD on the basis of the characteristics of traffic fluctuations and through integer optimization. The method exploits the characteristics of fluctuations in traffic flow to first separate traffic into free-flow and congested regimes, then applies a minimum principle to identify equilibrium states, and finally obtains a piecewise linear FD through integer optimization that minimizes the absolute error between observed and fitted equilibrium data points. The piecewise linear form is flexible enough to approximate any other FD form, and the method is adaptive and data driven.

Application of this method to three locations of a freeway in California indicates that a three-piece linear FD is adequate in obtaining a good fit to all but one data set. The single data set for which this method fails to separate the two flow regimes pertains to a location where flows from an entry ramp fundamentally change the flow characteristics of the right lane, where the transition from free-flow to congested flow is more gradual, and the fitted FD has a flatter top, a sign of the existence of a nearby bottleneck. Even in this case, a three-piece FD appears to fit the data reasonably well. The results also confirm several well-known traffic phenomena: the capacity drop (in the fast lane) and decreasing capacities from the left to the right lanes.

Although the use of a piecewise linear FD, when it is continuous and concave, greatly simplifies analysis of the kinematic wave traffic flow model, the existence of capacity drops, and nonconcavity observed in the empirical FDs present a challenge to the well-posedness of the kinematic wave model endowed with these FDs, which is worthy of further investigation.

REFERENCES

1. Zhang, H. New Perspectives on Continuum Traffic Flow Models. *Networks and Spatial Economics,* Vol. 1, No. 1, 2001, pp. 9–33.
2. Castillo, J., and F. Benítez. On the Functional Form of the Speed-Density Relationship I: General Theory. *Transportation Research Part B,* Vol. 29, No. 5, 1995, pp. 373–389.
3. Coifman, B. A. New Methodology for Smoothing Freeway Loop Detector Data: Introduction to Digital Filtering. In *Transportation Research Record 1554,* TRB, National Research Council, Washington, D.C., 1996, pp. 142–152.
4. Cassidy, M. Bivariate Relations in Nearly Stationary Highway Traffic. *Transportation Research Part B,* Vol. 32, No. 1, 1998, pp. 49–59.
5. Zhang, H. A Mathematical Theory of Traffic Hysteresis. *Transportation Research Part B,* Vol. 33, No. 1, 1999, pp. 1–23.
6. Windover, J., and M. Cassidy. Some Observed Details of Freeway Traffic Evolution. *Transportation Research Part A,* Vol. 35, No. 10, 2001, pp. 881–894.
7. Lighthill, M., and G. Whitham. On Kinematic Waves. II. A Theory of Traffic Flow on Long Crowded Roads. *Proceedings of the Royal Society of London. Series A, Mathematical and Physical Sciences,* Vol. 229, No. 1178, 1955, pp. 317–345.
8. Richards, P. Shock Waves on the Highway. *Operations Research,* Vol. 4, No. 1, 1956, pp. 42–51.
9. Newell, G. A Simplified Theory of Kinematic Waves in Highway Traffic, Part II: Queueing at Freeway Bottlenecks. *Transportation Research Part B,* Vol. 27, No. 4, 1993, pp. 289–303.
10. Daganzo, C. The Cell Transmission Model: A Dynamic Representation of Highway Traffic Consistent with the Hydrodynamic Theory. *Transportation Research Part B,* Vol. 28, No. 4, 1994, pp. 269–287.
11. Castillo, J., and F. Benítez. On the Functional Form of the Speed-Density Relationship II: Empirical Investigation. *Transportation Research Part B,* Vol. 29, No. 5, 1995, pp. 391–406.
12. Koshi, M., M. Iwasaki, and I. Ohkura. Some Findings and an Overview on Vehicular Flow Characteristics. *Proc., Eighth International Symposium on Transportation and Traffic Theory,* Toronto, Ontario, Canada, 1981, p. 403.
13. Hall, F. L., and K. Agyemang-Duah. Freeway Capacity Drop and the Definition of Capacity. *Transportation Research Record 1320,* TRB, National Research Council, Washington, D.C., 1991, pp. 91–98.
14. Jia, Z., C. Chen, B. Coifman, and P. Varaiya. The PeMS Algorithms for Accurate, Real-Time Estimates of G-Factors and Speeds from Single-Loop Detectors. *IEEE Control* Systems Magazine, Vol. 21, No. 4, 2001, pp. 26–33.
15. Dafermos, C. Polygonal Approximations of Solutions of the Initial Value Problem for a Conservation Law. *Journal of Mathematical Analysis and Applications,* Vol. 38, No. 1, 1972, pp. 33–41.
16. Nakayama, A., M. Fukui, K. Hasebe, M. Kikuchi, K. Nishinari, Y. Sugiyama, S. Tadaki, and S. Yukawa. Detailed Data of Traffic Jam Experiment. In *Traffic and Granular Flow '07,* Springer, New York, 2009, pp. 389–394.
17. Tadaki, S., M. Kikuchi, A. Nakayama, K. Nishinari, A. Shibata, Y. Sugiyama, and S. Yukawa. Scale-Free Features in the Observed Traffic Flow. In *Traffic and Granular Flow '05,* Springer, New York, 2007, pp. 709–715.
18. Mauch, M., and M. Cassidy. Freeway Traffic Oscillations: Observations and Predictions. *Proc., 15th International Symposium on Transportation and Traffic Theory,* Adelaide, Australia, 2002.
19. Ahn, S. *Formation and Spatial Evolution of Traffic Oscillations.* PhD thesis. University of California, Berkeley, 2005.
20. Li, X., F. Peng, and Y. Ouyang. Measurement and Estimation of Traffic Oscillation Properties. *Transportation Research Part B,* Vol. 44, No. 1, 2009, pp. 1–14.
21. Hu, K., P. Ivanov, Z. Chen, P. Carpena, and H. E. Stanley. Effect of Trends on Detrended Fluctuation Analysis. *Physical Review E,* Vol. 64, No. 1, 2001, p. 11114.
22. Bertsimas, D., and R. Shioda. Classification and Regression via Integer Optimization. *Operations Research,* Vol. 55, No. 2, 2007, pp. 252–271.

The Traffic Flow Theory and Characteristics Committee peer-reviewed this paper.